Real time ultrasound assessment of contact progress between food gels and tongue mimicking surfaces during a compression

Mathieu Mantelet, Rohit Srivastava, Frederic Restagno, Isabelle Souchon, Vincent Mathieu

Real time ultrasound assessment of contact progress between food gels and tongue mimicking surfaces during a compression

Mathieu MANTELET[a], Rohit SRIVASTAVA[a], Frédéric RESTAGNO[b], Isabelle SOUCHON[c] and Vincent MATHIEU[a]

[a] Université Paris-Saclay, INRAE, AgroParisTech, UMR SayFood, F-78850, Thiverval-Grignon, France

[b] Université Paris-Saclay, CNRS, Laboratoire de physique des solides, 91400 Orsay, France

[c] INRAE, Avignon Université, UMR408 SQPOV, F-84000 Avignon, France

Submitted to ***Food Hydrocolloids***

Declarations of interest: none.

Corresponding author:

Vincent Mathieu

Paris-Saclay Food and Bioproduct Engineering Research Unit (SayFood UMR 782)

Joint Research Unit INRAE AgroParisTech

Bâtiment CBAI

1, avenue Lucien Brétignières

78850 Thiverval-Grignon, France

Mail: vincent.mathieu@inrae.fr

Phone: +33(0)1 30 81 68 13

Fax: +33(0)1 30 81 55 97

Abstract

An *in vitro* study was conducted to further explore the potential of an emerging ultrasound method for monitoring in real time the progress of the contact between gels with different physical properties and tongue mimicking surfaces (TMSs) during uniaxial compressions. A 1-MHz ultrasound transducer was used to measure the apparent reflection coefficient (R^*) of the interface between TMSs (of varied roughness) and gels (agar and/or gelatin). The patterns of R^* clearly depended on the gels capacity to deform and mould the asperities of the TMSs during compression. Rough TMSs induced a significant decline of R^* values, demonstrating an increase of the fraction of the TMSs in direct contact with the gels. Rigidity, fracture properties or adhesion energy of gels influenced the kinetics of contact progress and associated patterns of R^* variations. Moreover, the presence of a thick lubrication film between the gels and the TMSs promoted the transmission of ultrasound waves (acting as a coupling agent) and led to decreasing values of R^*. Such phenomena were observed both when depositing a water lubrication film of controlled thickness on the TMSs (to mimic salivary film) and when considering gels with high water release capacities. The study confirms the potential of ultrasound methods for exploring physical phenomena related to interactions between food and tongue surface. Such developments could better contribute to unravel the determinants of texture perceptions during food oral processing.

Key words

Oral processing; Tongue; Roughness; Agar; Gelatin; Ultrasound

1. Introduction

1.1. Role of the tongue in food oral processing and texture perceptions

Food oral processing plays a major role in consumers' appreciation of food as it encompasses dynamic, multi scale and multi-sensory perceptions. Food is subjected to multiple biomechanical and chemical processes in oral cavity (Hutchings & Lillford, 1988; Stokes et al., 2013). It is chewed by the teeth, moistened by the saliva, mixed and sheared by the action of the tongue, the palate and the cheeks, adjusted to suitable oral temperature, so that it can be transformed into a bolus ready to be swallowed in safe and comfortable conditions (Hiiemae, 2004). Each one of these actions leads to the stimulation of sensory receptors that make it possible to monitor the changes in ingested food during oral processing.

Even if the consumer needs to adapt his or her strategy of oral processing to the wide diversity of food structures, the manipulation of food between the tongue and the palate is a step required for every food products and at every moment of oral processing. The dynamic physical interactions at tongue-food interface give rise to the activation of various mechanoreceptors located in tongue, and which highly contribute to the perception of food texture (Bukowska et al., 2010). Since the tongue plays such a crucial part in the sensory experience of the consumer, a better understanding of texture perceptions resulting from tongue-food-palate interactions may provide important benefits for the design of new foods with improved sensory properties.

Moreover, the tongue also makes it possible to evaluate in real time the changes of the mechanical status of the bolus in order to decide the most appropriate moment for triggering a safe swallowing sequence (J. Chen, 2009; Hutchings & Lillford, 1988). Precisely, understanding the mechanisms of texture perceptions between the tongue and the palate could be helpful for the design of an alternative food supply for specific populations facing swallowing disorders (dysphagia). The response to this challenge requires the unraveling of the dynamic structural and mechanical

71 transformations undergone at tongue-food interface during oral processing (Foegeding et al., 2017;
72 Hutchings & Lillford, 1988; Panouillé et al., 2016; Szczesniak, 2002).

73 1.2. Need for in-situ and dynamic instrumental characterizations

74 The development of technical approaches is essential for exploring the physical phenomena
75 involved in texture perceptions. Numerous studies have attempted to mimic some specific sequences
76 of food oral processing with mechanical testing or rheological approaches (J. S. Chen & Stokes, 2012).
77 Even though these technics are suitable for the characterization of the transformations in the bulk of
78 food, they do not make it possible to comprehend the physical information related to the surface
79 properties, which are critical for tactile mechano-sensations. Tribology has also been proposed as an
80 effective tool to describe, at the end of oral processing or right after swallowing, the friction
81 mechanisms due to the interaction between the surface of the tongue and food bolus (Stokes et al.,
82 2013). However, from the introduction in the oral cavity to swallowing, food undergoes major
83 transformations, in such a way that oral processing goes from rheology to tribology dominant phases.
84 As a consequence, the development of *in-situ* and non-destructive methods suitable for the
85 continuous evaluation of the different phases of oral processing represents a critical research gap
86 (Foegeding et al., 2017).

87 1.3. The potential of ultrasound techniques

88 Ultrasound (US) methods could help to address this challenge. US imaging has already been
89 used in the oral cavity for various applications, including the study of food bolus transportation during
90 swallowing (de Wijk et al., 2011; Galén & Jost-Brinkmann, 2010; Peng et al., 2000), of tongue shape
91 and motions during speech (Stone, 2005), of functional disorders such as dysphagia (Hsiao et al., 2012;
92 Kim & Kim, 2012; Rommel & Hamdy, 2016) or also of obstructive sleep apnea events (J.-W. Chen et al.,
93 2014; Chien et al., 2017; Weng et al., 2017). The wide diversity of these fields of application confirms
94 the capability of US methods for the real-time exploration of dynamic mechanisms in oral cavity.

Furthermore, ultrasound waves are sensitive to the physical properties of the media and interfaces they propagate through. For instance, ultrasound technics have thus been proposed to characterize food composition, structure, or transformation processes in various products such as meat, fruits, vegetables, emulsions or gels (Awad et al., 2012).

A first exploratory study has investigated the variations of the apparent reflection coefficient (referred to as *R** hereafter) of ultrasound waves at the interface between non-deformable tongue mimicking surfaces (TMS hereafter) and agar/gelatin mixed gels with various physical properties (Mantelet et al., 2020). The results have shown that the US method has a high potential for the characterization of the capability of food gels to mold themselves into the surface asperities. The properties of both TMS*s* (roughness, lubrication) and food (Young's modulus, syneresis) were shown to have an impact on *R** values. In static conditions, the apparent reflection coefficient was significantly larger in the following situations: (i) tongue asperities were high and dense; (ii) lubrication levels were low; and (iii) gels were less rigid. The apparent reflection coefficient conveyed the ability of food gels to mold themselves to surface asperities or to form a coupling film of liquid at the interface. These preliminary experiments were conducted in static conditions, with the aim to mimic the initial contact between food and the surface of the tongue. However, no mechanical load was applied to the food samples and it is now required to go further and investigate the behavior of the US response of the system during the break down of food.

For that purpose, the present study aims at investigating the evolution of *R** during a uni-axial compression mimicking the initial step of food oral processing. The same TMS*s* and model gels as those considered in the first study have been used to explore the impact of their respective properties on the variations of *R** (Mantelet et al., 2020).

2. Material and Methods

2.1. Model foods

Eight food gels identical to those previously considered for static conditions were prepared following the same protocol (Mantelet et al., 2020). These gels are composed of agar (HP700IFG, Kalys, Bernin, France) and gelatin (Bloom 250 PS 8/3, Rousselot, Gent, Belgium), sucrose (Daddy, Cristalco, Paris, France) and water. For one of the eight samples Tween 20 (CAS: 9005-64-5 FG, Sigma-Aldrich, St Louis, MO, USA) emulsifier was used to alter sample's surface wettability. All the gels underwent identical thermal treatments, so that to dissolve sucrose, agar and gelatin at different heating steps. Firstly, solutions of water with sucrose were prepared and stirred for 30 min at room temperature (20°C). Secondly, agar powder was incorporated (if required) and all solutions were heated to 100°C, ensuring the complete dissolution of agar. Thirdly, solutions were cooled and stabilized for 5 min to 60°C. Lastly, gelatin powder was added (for gels with gelatin) and all solutions were stirred for 20 min at 60°C. Solutions at 60 °C were then poured in polyethylene cylindrical molds and left at 19 °C during 15 h-18 h. The gels cylinders of 30 mm in diameter and 10 mm in height were individually unmolded at the last moment before the experiments. The gels can be classified in two main categories: $Ag_{0.3}$, $Ag_{1.8}$ and $Ag_1Ge_{0.75}$ are agar dominant samples, whereas $Ge_{3.5}$, $Ag_{0.3}Ge_{3.5}$, $Ag_{0.7}Ge_{5.85}$, Ge_7 and Ge_7T are gelatin dominant samples. It is important to note that Ge_7T differs from Ge_7 only by the presence of Tween 20. Introducing this emulsifier led a to a decrease of the contact angle (from 40 to 0°) (Mantelet et al., 2019). The underlying objective was to investigate whether the wettability of the gels is likely to influence the patterns of due to differences in water film spreading at the interface between the TMS and the food. Table 1 summarizes, for each of the eight gels considered here, the type of dominant polymer, the composition and the Young's modulus obtained from previous characterizations (Mantelet et al., 2020).

2.2. Tongue mimicking surfaces

As in our previous study, three cylinders of PVC (polyvinyl chloride) were used as TMSs (Mantelet et al., 2020). The diameter of the PVC cylinders (50 mm) was kept larger than that of model foods in order to ensure that they fully rest on the TMSs. The height of the cylinders (20 mm) was

chosen to be in accordance with the acoustic properties of PVC (Mantelet et al., 2020). Three types of TMSs were used in this study, with different surface roughness characteristics imprinted by sand papers during the course of cylinder moulding. Referred to as $R_0\beta_0$, $R_1\beta_1$ and $R_1\beta_2$, the TMSs differ specifically by their arithmetical mean height *Ra* (mean ± standard deviation of the height of the asperities, respectively equal to 2.5±0.1, 58.2±5.3 and 52±11.2 µm) and by their correlation length β (related to the density of the asperities and respectively, with mean ± standard deviation equal to 35±0.4, 206±4 and 243±12 µm). Both the above mentioned parameters were obtained through profilometry measurements and were found to be reproducible for each TMS production (Mantelet et al., 2020). The mean height of the asperities on the surface of real tongues has been estimated to range from 40 and 100 µm, showing that $R_1\beta_1$ and $R_1\beta_2$ displayed physiological relevant values (Uemori et al., 2012). Conversely, $R_0\beta_0$ can be considered as smooth when compared to $R_1\beta_1$, $R_1\beta_2$, or to real tongues. This TMS can thus be used as a control, making it possible to discuss the impact of surface roughness with negligible effects of contact progress between the gels and the TMSs.

For the sake of simplicity, water was used as a lubricant to mimic the lubrication of the tongue surface by saliva. Four lubrication levels were considered, referred to as dry, low, medium and high (Mantelet et al., 2020). Dry (absence of lubricant) and high (water film of 1 mm thick) levels were voluntarily chosen to compare highly contrasting conditions. The high lubrication level is much higher than orders of magnitude of salivary film thickness. This condition made it possible to ensure that water was the only medium present at the interface between the food and the TMS. The underlying objective was to investigate whether the wettability of the gels is likely to influence the ultrasound response at the interface between the TMS and food, due to potential differences in water film spreading at the interface. Low and medium levels correspond to 15 and 40 µm thick water films respectively, deposited on the TMS with a spray in a controlled and reproducible way.

2.3. Compression protocol

A tension-compression machine (TA.XT plus, stable Micro System, Surrey, United Kingdom) was used to simulate the tongue/palate compression (see Figure 1). The TMS was mounted on the base of the apparatus, while a circular aluminum probe (diameter 40 mm) was used to play the role of the hard palate. The food samples underwent 80 % uni-axial compressions at 10 $mm.s^{-1}$, which was the highest value of velocity attainable with the set-up. The compression protocol was composed of different steps.

Firstly, before each test, the TMS was cleaned with a dish soap (Liquide Vaisselle Main Ecologique, Prop, Paris, France) and dried. The TMS was then lubricated following one of the four conditions described above. The food sample to be tested was unmoulded and deposited on the TMS right before the experiment, to prevent any syneresis, drying and sagging over time. Then, the mimicking palate was put in contact with the food sample and the following compression sequence was applied: a static holding step of 3 s at 0 % strain, followed by a compression step of 80 % at 10 $mm.s^{-1}$, and finally a second holding step of 3 s.

The experiments were conducted at room temperature (mean ± standard deviation equal to 19±1 °C), and at least in triplicate (and up to four times) for each set of conditions (*i.e.*, for a given food gel on a TMS of a given roughness and with a given lubrication level).

2.4. Ultrasound measurements

The ultrasonic measurements aim at monitoring the evolution of R^* during the compression of the different food gels on the bio-mimicking set up described above. The device and the procedure used for ultrasound measurements is the same as in our previous paper (Mantelet et al., 2020).

2.4.1. Ultrasonic device

The device was composed of a mono-element piezoelectric transducer (V103RM, Olympus, Shinjuku, Tokyo, Japan) with a central frequency of 900 kHz (longitudinal waves). The US transducer was positioned underneath the TMS (silicon grease was used as coupling agent). The transducer was

connected to a US pulser-receiver (Sonatronic, Evry, France), which produced a negative squared pulse signal (500 ns width, 80 Volt amplitude) for the emission of the US pulse, and which digitalized the radio frequency (*rf*) signals corresponding to the pulse echo response of the system (12-bit quantification, 100 MHz sampling rate, 38 dB gain). The acquisition of the *rf* signals was done in real time during the compressing tests using a dedicated user-interface developed with LabVIEW® (LabVIEW, National Instrument, Austin, Texas, USA). The pulse recurrence frequency was of around 90 Hz. The typical number of signals acquired during a compression was of around 70.

2.4.2. Signal processing

The sets of *rf* signals obtained for each compression test were processed with MATLAB® (The MathWorks, Natick, Massachussetts, USA). *R** was calculated for each individual *rf* signal, following the protocol extensively described in our previous study (Mantelet et al., 2020). To summarize it briefly, the first step consisted of high-frequency noise reduction with a low-pass filter (15 MHz cutoff frequency) applied to the Fast Fourier Transform (FFT) of the *rf* signals. The *rf* signals were composed of two main echoes (see Figure 1.b): E_0 corresponds to the acoustic energy reflected at the interface between the TMS and the food gel, whereas E_1 is the response of the interface between the food gel and the palate. During the uniaxial compression (see Figure 1.c), the time of flight of E_1 decreases and tends to get closer to E_0. The present study focuses on E_0 but some undesired artefacts may occur by the end of the compression due to overlapping between E_0 and E_1. Time intervals of interest (4 µs width) centered on the maximum of the modulus of the Hilbert transform of echo E_0 (see Figure 1.b) were determined to track the echo of the TMS. The amplitude A_0, defined as the modulus of the FFT of these temporal windows at 900 kHz, was then calculated for each *rf* signal. Finally, *R** was obtained following:

$$R^*(\varepsilon) = \frac{A_0(\varepsilon)}{A_{0,\mathrm{ref}}} \qquad \text{Eq 1}$$

Where ε is the ratio of compression displacement to initial gel height (ranging from 0 to 80 %) corresponding to each *rf* signal and $A_{0,ref}$ is a reference value of the amplitude A_0 recorded before lubricating the TMS and depositing the food sample.

For better interpretation, the variations of *R** during the compression were also compared to their initial value and *ΔR** is defined as follows:

$$\Delta R^*(\varepsilon) = R^*(\varepsilon) - R^*(\varepsilon = 0) \quad \text{Eq 1}$$

In this way, it becomes easier to compare and analyze the amplitude of the variations of *R** across the different experimental conditions.

3. Results and discussion

The results and discussion are structured in three distinct subsections, so that to discuss successively the impact of (i) tongue roughness, (ii) food properties and (iii) tongue lubrication on the variations of *R** during the compression of the food gels on TMSs. For all figures, the curves with identical colors correspond to replicates of identical conditions.

3.1. Impact of surface roughness on *R**

Figure 2.a represents the values of *R** before the compression (ε = 0) of the gels $Ag_{0.3}$, $Ge_{3.5}$, Ge_7 on the three TMSs $R_0\beta_0$, $R_1\beta_1$, and $R_1\beta_2$ (in absence of lubrication). The three food gels selected here provide an overview of the various behaviors observed throughout the whole set of food samples. In the case of the smoothest TMS ($R_0\beta_0$), similar values of *R** were reported across the three food samples (around 33%). Contrarily, the presence of rough asperities on $R_1\beta_1$, and $R_1\beta_2$ led to higher and dispersed values of *R** across the three gels. The apparent reflection coefficient of US waves crossing the TMSs depends on the gap of acoustic impedance *Z* between the TMSs ($Z \simeq 3.1$ MPa.s.m-1 in PVC) and surrounding media (Mantelet et al., 2019). In the present case, the surrounding media can be composed of air ($Z \simeq 420$ Pa.s.m-1), food gels (*Z* laying from 1.6 to 1.75 MPa.s.m-1) or of water ($Z \simeq$ 1.5 MPa.s.m-1) (Mantelet et al., 2019). Air has a negligible acoustic impedance when compared to PVC,

food gels and water (the two latter being similar). The higher the gap of acoustic impendance at the interface, the higher amplitude of US echo E_0 and subsequent value of R^*. If air fully covers a TMS, we are in the case of a full reflection of the US wave and R^* is close to 100%. If contrarily the TMS is fully imprinted with gels, R* has been show to range from 30 to 34%, depending on the acoustic impedance of the different gels (related to both mass density and compressibility) (Mantelet et al., 2019). When a food sample is deposited on the TMS, a mix of air and gel in direct contact with the TMS is observed, with intermediate values of R^*. Consequently, R^* has been shown to be an indirect indicator of the effective contact ratio between the food gel and the TMS (Mantelet et al., 2020). As a consequence, Figure 2.a highlights that prior to the uni-axial compression, the surface $R_0\mathcal{B}_0$ displayed a better mechanical coupling with the food gels than the two other surfaces ($R_1\mathcal{B}_1$ and $R_1\mathcal{B}_2$).

Concerning ΔR^*, an increase of ΔR^* during the compression of the gels means a spreading of the surface of air in direct contact with the TMS. Conversely, a decrease of ΔR^* means that the surface of gel or water in direct contact with the TMS tends to increase. Figure 2.b shows the variations of ΔR^* during a compression test for the same gels and TMSs (no lubrication). In the case of the smoothest TMS ($R_0\mathcal{B}_0$), no apparent variations of ΔR^* were reported during the compression of the different gels (blue curves in Figure 2.b), except in some cases at higher strains (higher than 70%). As pointed out previously (Figure 1.c), the possibility of E_1 to overlap with E_0 at the end of the compression sequence might be responsible for this observed abnormal variation of amplitude at higher strains. Setting aside these undesired artefacts, the results suggest that the contact surface between the TMS $R_0\mathcal{B}_0$ and food was not altered during the compression tests. For these three gels, R^* was shown to range between 33 and 34 % before the beginning of the compression (see Figure 2.a), suggesting a full contact between the TMS and the food.

Contrarily to $R_0\mathcal{B}_0$, variations of ΔR^* were observed for the rough TMSs $R_1\mathcal{B}_1$ and $R_1\mathcal{B}_2$ during the compression (see Figure 2.b). These results suggest that the nature of the media in direct contact with the asperities of the TMSs varies when the food gel is under load. Interestingly, different trends

were observed throughout the three gels in Figure 2.b. For gels $Ge_{3.5}$ and $Ag_{0.3}$, a slight increase of US reflectivity was first observed, followed by a decreasing trend during the second portion of the compression. However, for these two gels, no major differences were observed between $R_1\mathcal{B}_1$ and $R_1\mathcal{B}_2$. The largest variations of ΔR^* were reported for Ge_7, which subsequently decreased by 15% after 80% strain (see Figure 2.b$_1$). Interestingly, a faster decrease was observed on $R_1\mathcal{B}_1$ at the beginning of the compression but later attaining the similar position as $R_1\mathcal{B}_2$ by the end of compression.

This result suggests that tongue roughness parameters may influence the evolution of the contact between the food gel and the asperities of the TMSs. $R_1\mathcal{B}_1$ and $R_1\mathcal{B}_2$ have similar values of R_a (average value of the height of asperities) and mainly differ by their correlation length $\mathcal{B}$ which suggests a higher density of surface asperities for $R_1\mathcal{B}_1$ than for $R_1\mathcal{B}_2$. As a consequence, the geometry of surface asperities may have an impact on the pattern of ΔR^* evolution during the compression. However, the gap of R^* at the end of the compression was similar to what it was at the beginning (around 12% higher for $R_1\mathcal{B}_1$ than for $R_1\mathcal{B}_2$).

3.2. Impact of food properties on R^*

The food gels considered in the present study mainly differ by the composition of their agar/gelatin ratio. Due to phase separation mechanisms between agar and gelatin (Clark et al., 1983; McEvoy et al., 1985), the gels can be arranged in two groups: gelatin dominant gels consisting in a continuous phase of gelatin with, if appropriate, agar inclusions ($Ge_{3.5}$, $Ag_{0.3}Ge_{3.5}$, $Ag_{0.7}Ge_{5.85}$, Ge_7), and conversely agar dominant gels composed of a continuous phase of agar with, if present, inclusions of gelatin ($Ag_{0.3}$, $Ag_1Ge_{0.75}$, $Ag_{1.8}$). Our previous study made it possible to show that for each type of samples, the higher the Young's modulus, the lower the capacity of the gels to mold the asperities of the TMS under the action of their own weight (without any imposed compression in that study), and the higher the apparent reflection coefficient R^* (Mantelet et al., 2020). This is clearly related to the link between the materials rigidity and the transition from a partial to a full contact (Degrandi-Contraires et al., 2013). However, the rigidity of the food samples is not sufficient to explain the

287 variations of R^*. As an example, $Ag_{0.3}$ and $Ge_{3.5}$ had similar values of rigidity but different values of R^*
288 prior to their compression. The adhesive energy of the food gels on the surface of PVC may be a
289 contributing factor to the capacity of the gels to mold themselves into the asperities of the TMSs. Such
290 properties are likely to vary according to the nature of the dominating polymer and to its level of
291 concentration (Shull, 2002). The potential role of water release mechanisms (acting as a coupling
292 media at the interface between the gel and the TMS and promoting the transmission of the US waves)
293 was also considered to explain the different behaviours reported for the two groups of samples. For
294 equal Young's moduli, the structure of agar dominant samples (double helix) could be more favorable
295 to the release of free water (syneresis) than the one of gelatin dominant samples (triple helix). Such
296 expelled water could act as a coupling media with the TMS and lead to lower values of R^* for agar than
297 for gelatin dominant samples (Santagiuliana et al., 2018). Once the water is released into the interface,
298 the adhesion forces get disrupted, making syneresis the prominent factor.

299 Figure 3.a shows the variations of the applied force F during the compression of the four gelatin
300 dominant gels. For these same gels, Figure 3.b displays the variations of ΔR^* on the same deformation
301 scale, while Figure 3.c represents the initial values of $R^*(\varepsilon=0)$ as a function of the Young's moduli of
302 the samples. Similarly, Figure 4 displays the same parameters as in Figure 3, but for agar dominant
303 gels: F versus ε in Figure 4.a, ΔR^* versus ε in Figure 4.b, and $R^*(\varepsilon=0)$ versus E in Figure 4.c. The results
304 given in Figure 3 and Figure 4 were obtained with the TMS $R_1\beta_1$, and for the dry lubrication level.

305 $Ge_{3.5}$ was the gelatin dominant gel with the lowest level of concentration in biopolymer (and
306 consequently with the lowest Young's modulus – 2.2 kPa). It also displayed the lowest level of variation
307 of ΔR^*, suggesting that during the compression, the amount of direct contact between the asperities
308 of the TMS and the food did not deviate from the initial level. By adding only 0.3 % of agar (in
309 comparison with $Ge_{3.5}$), $Ag_{0.3}Ge_{3.5}$ displayed larger evolutions of ΔR^*, with a slight increase during the
310 first step of the compression, generally followed by a decrease, until recovering their initial values (ΔR^*
311 comprised between -2 and +5% at the end of the compression). However, disparate behaviors were

displayed across the four trials repeated for $Ag_{0.3}Ge_{3.5}$, suggesting that for this sample, the presence of agar inclusions led to heterogeneous variations of the conditions of the contact with the TMS. The two last gelatin dominant gels had a significantly higher Young's moduli (32.1 and 24.0 kPa for $Ag_{0.7}Ge_{5.85}$ and Ge_7 respectively). Both model food displayed declining trends of ΔR^* variations at the end of the compression (by 7 to 10 and 12 to 14 % for $Ag_{0.7}Ge_{5.85}$ and Ge_7 respectively). For $Ag_{0.7}Ge_{5.85}$, which was the most rigid, this decline of ΔR^* was faster at the beginning of the compression (between 0 and 15 % strain), followed by an increase at the very end of the compression (beyond 75 % strain). The increase at the end coincides with the decrease reported on the force curve, which allows us to identify the fracture of the food sample.

Now when we consider agar dominant samples (see Figure 4), it is noticeable that $Ag_{0.3}$ did not go through significant variations of F and ΔR^* during the compression. Due to the low rigidity of $Ag_{0.3}$ (E = 4.2 kPa), the amplitude of the load transmitted to the interface during the compression may not have been high enough so that to alter the nature of the media in direct contact with the TMS. Moreover, the low values of R^* reported before the beginning of the compression ($R^*(\varepsilon=0)$ = 45.9 %) indicate that even before the beginning of the compression, the coupling between the food and the TMS was already close to the threshold, providing a very little scope for further improvement. Although, distinct force-deformation curves were reported for more rigid gels like $Ag_1Ge_{0.75}$ and $Ag_{1.8}$, with fracture occurring between 45 and 55%. A rapid decrease of ΔR^* was observed in the first part of the compression (before 40 % deformation), all the more so when the Young's modulus of the sample was high (between 10 and 18 % for $Ag_1Ge_{0.75}$ while between 24 and 28 % for $Ag_{1.8}$). During this first half of the compression, analogous patterns of ΔR^* were displayed inside the different food references. These tendencies suggest that a significant increase of the amount of gels in contact with the TMS occurred during the first part of the compression. After 40 % strain, the ΔR^* curves exhibit more individual behaviors, each showing an increase of R^* that reflects relaxation mechanisms leading to the withdrawal of the food sample from the asperities of the TMS.

3.3. Impact of surface lubrication on *R**

The experiments depicted in the first two parts of this discussion focused on investigating the behavior of *R** in absence of lubrication at the interface between the TMS and the food. However, accounting for lubrication is also a critical issue for seeking to understand the role of the salivary film at this interface. In this feasibility study, a particular importance was granted to working with a stable and reproducible fluid, reason why water was preferred over real saliva. A recent work by our group displayed that in absence of mechanical loading (other than gravity), the lubrication of the TMS with water drastically affects the US response of the interface (Mantelet et al., 2020).

Ge_7 and Ge_7T were chosen to illustrate the effect of the lubrication of the TMS during a compression. These two samples differ by the presence of Tween 20 in Ge_7T, an emulsifying agent used to modify surface tension properties (all by keeping the elastic properties unchanged in comparison with Ge_7). For the four lubrication conditions, Figure 5 shows the variations of ΔR^* as a function of strain for Ge_7 (Figure 5.a_1 and 5.b_1) and Ge_7T (Figure 5.a_2 and 5.b_2). Two distinct surface profiles were considered: $R_0\mathcal{B}_0$ for Figures 5.a_1 and 5.a_2, $R_1\mathcal{B}_2$ for Figures 5.b_1 and 5.b_2.

Lower decrement rates of ΔR^* were reported during the compression of Ge_7 on the TMS $R_0\mathcal{B}_0$ (mostly comprised between -0.2 and -1%), with no specific patterns underscored across the four lubrication conditions. On the same TMS $R_0\mathcal{B}_0$, slightly higher decreases were displayed with Ge_7T: between 0 and -1.2% for most of the tests, and as low as between -2 and -4% in some isolated cases which were not related to a specific lubrication condition. For both samples, the initial value of *R** was inferior to 40%, suggesting that even before the beginning of the compression, the food gels were almost fully bonding the interface of the TMS. As a consequence, the margin available for improving the contact during the compression was low, explaining why low variations of ΔR^* were displayed.

Different trends of variations were reported throughout the four lubrication conditions for the profile $R_1\mathcal{B}_2$.

The dry lubrication level led to the highest variations of ΔR^*, with a decrease by -8 to -10% for Ge_7 and by -13 to -16% for Ge_7T. These observations suggest a significant improvement of the acoustic coupling at the interface between the TMS and the food. Interestingly, the initial value of R^* was lower for Ge_7T (mean ± standard deviation equal to 63.6±0.4%) than for Ge_7 (mean ± standard deviation equal to 68.1±2.3%). As a consequence, Ge_7T displayed a higher capacity to fill the asperities of the TMS during the compression. A reason for these tendencies could be that Tween 20 may promote the adhesive properties of Ge_7T, then altering the balance between adhesive and elastic forces that are jointly ruling the interaction between the food and the TMS.

Conversely, the high lubrication level led to the lowest variations of ΔR^*, with a slightly linear decrease (between -1 and -2% both for Ge_7 and Ge_7T). Lower initial values of R^* (before the beginning of the compression) suggest a homogeneous coupling between the gels and the TMS, and hence provided limited scope of further improvement during the compression. In this case, the film of water (with an acoustic impedance similar to that of gels) acts as a coupling agent and fills the asperities of the TMS. The results in Figure $5.b_1$ and $5.b_2$ suggest that when a load is applied to the food sample during the compression, the film of water at the interface does not affect the coupling at the interface.

With relevance to the physiological orders of magnitude of the salivary film thickness (Pramanik et al., 2010), the low and medium levels of lubrication made it possible to observe how the patterns of ΔR^* evolve between dry and high levels. For both levels, ΔR^* first displayed a slight increase, before a more pronounced decrease during the second portion of the compression. The curves related to low and medium levels followed similar trends for most of the compression sequences. It was only at the end of the compression that lower values of ΔR^* were observed for the low level (in a more prominent way for Ge_7T). Even though the difference of water film thickness between low and medium levels is small, one can notice that it is large enough to detect changes in the US response that are induced by the spreading of the lubricating film at the interface between the food and the TMS. In particular, for the low level, the higher wettability of Ge_7T compared to Ge_7

(contact angles previously assessed: around 0° and 40° respectively (Mantelet et al., 2019)) was likely to promote the spreading of the lubricating film, which may contribute to the explanation of the higher decrease rate of ΔR^* reported for this sample.

4. Conclusions

In this study, non-deformable surfaces were considered as TMSs to study the impact of surface roughness and lubrication on the variations of R^* during the compression of different food gels with different physical properties.

The findings show that both the height and the width of the asperities on the TMSs induces high variations of the apparent reflection coefficient during the compression of the gels, corresponding to the progressive molding of food into the surface asperities of the TMSs. Highly diverse patterns were displayed across the different food gels. Rigidity of gels was also found to impact the kinetics of increase of direct contact area between TMSs and gels. Moreover, two specific trends of behavior have been reported depending on whether the dominant polymer in gels was agar or gelatin. The results suggested that agar dominant products had higher capability for water release or syneresis during the compression. This syneresis phenomenon was observed with the ultrasound method as it led to the formation of a coupling film at the interface between the TMS and the food, resulting in a decrease of the US reflectivity. For the same reasons, lubrication with water at the interface between the gels and the TMSs tended to mitigate the evolution profiles of R* during a compression.

In the context of food oral processing, the apparent reflection coefficient could help to understand how food gels mold themselves into the surface asperities of the tongue, or how a coupling film of liquid at the interface between the food and the tongue may spread. The method has thus a potential for providing an indirect estimation of the contact area between the tongue surface and food, which would be worthwhile for clarifying the mechanisms underlying sensory perceptions during oral processing (Ares et al., 2007; Szczesniak, 2002). Such an approach could indeed help understanding how the mechanical loads can be transmitted to the mechanoreceptors in the vicinity

411 of tongue asperities (e.g. in relation with firmness sensations), how the interactions of food and the
412 salivary film with tongue asperities may rule the perceptions of moistness, or also how the fraction of
413 tongue surface in contact with food influence the diffusion of chemical compounds responsible for
414 taste perceptions on tongue surface.

415 However, much more work will need to be done before being able to judge the applicability of
416 our method for such issues. In this view, many physiological issues will need to be accounted for,
417 starting with considering deformable tongue mimicking samples and progressively moving to more
418 realistic motions (involving both compressional and shear motions). All along these improvements, the
419 method should bring new insights for unravelling the determinants of texture perceptions during the
420 manipulation of food between the tongue and the palate.

421 The shearing of food between the tongue and the palate gives rises to important texture
422 perceptions, particularly for understanding swallowing trigger points. Characterizing the thickness of
423 food samples in tongue-palate tribo-pair is a critical missing information for the identification of the
424 lubrication regime of the system (Rudge et al., 2019). In future work, we could also try to investigate
425 whether an ultrasound method could be used in order to reach this objective.

426 A longer term perspective could be to extend the development of the method to *in vivo*
427 applications, with measurements conducted directly on the consumer. Finally, a broader diversity of
428 more realistic food types should be considered (e.g., with irregular shapes and micro or macroscopic
429 structural heterogeneities), and the evolving properties of the food bolus during oral processing should
430 also be examined (e.g., particle size reduction, saliva incorporation).

431 ## Acknowledgments

432 We wish to acknowledge Jean-Luc Gennisson for the detailed advice he provided on the
433 ultrasound analyses. We are grateful to David Forest, Claire Juguet, Raphaëlle Ponthieux, and Gabriel

434 Debar for their crucial technical support. We also warmly thank Sandrine Mariot for her help with
435 profilometry measurements.

436 Funding

437 This work was financially supported by (i) the IDI 2015 project funded by IDEX Paris Saclay
438 (ANR-11-IDEX-0003-02), (ii) the PLUS project funded by the French National Institute for Agriculture,
439 Food and Environment (INRAE, 2015), and (iii) the QUSToFood project funded by the French National
440 Research Agency (ANR-17-CE21-004).

Bibliography

Ares, G., GonçAlvez, D., PéRez, C., ReolóN, G., Segura, N., Lema, P., & GáMbaro, A. (2007). Influence of gelatin and starch on the instrumental and sensory texture of stirred yogurt. *International Journal of Dairy Technology*, *60*(4), 263–269. https://doi.org/10.1111/j.1471-0307.2007.00346.x

Awad, T. S., Moharram, H. A., Shaltout, O. E., Asker, D., & Youssef, M. M. (2012). Applications of ultrasound in analysis, processing and quality control of food: A review. *Food Research International*, *48*(2), 410–427. https://doi.org/10.1016/j.foodres.2012.05.004

Bukowska, M., Essick, G. K., & Trulsson, M. (2010). Functional properties of low-threshold mechanoreceptive afferent in the human labial mucosa. *Experimental Brain Research*, *201*(1), 59–64. https://doi.org/10.1007/s00221-009-2005-0

Chen, J. (2009). Food oral processing—A review. *Food Hydrocolloids*, *23*(1), 1–25. https://doi.org/10.1016/j.foodhyd.2007.11.013

Chen, J. S., & Stokes, J. R. (2012). Rheology and tribology: Two distinctive regimes of food texture sensation. *Trends in Food Science & Technology*, *25*(1), 4–12. https://doi.org/10.1016/j.tifs.2011.11.006

Chen, J.-W., Chang, C.-H., Wang, S.-J., Chang, Y.-T., & Huang, C.-C. (2014). Submental ultrasound measurment of dynamic tongue base thickness in patients with obstructive sleep apnea. *Ultrasound in Medicine & Biology*, *40*(11), 2590–2598. http://dx.doi.org/10.1016/j.ultrasmedbio.2014.06.019

Chien, C.-Y., Chen, J.-C., Chang, C.-H., & Huang, C.-C. (2017). Tracking dynamic tongue motion in ultrasound images for obstructive sleep apnea. *Ultrasound in Medicine & Biology*. http://dx.doi.org/10.1016/j.ultrasmedbio.2017.08.001

Clark, A. H., Richardson, R. K., Ross-Murphy, S. B., & Stubbs, J. M. (1983). Structural and mechanical properties of agar/gelatin co-gels. Small-deformation studies. *Macromolecules*, *16*(8), 1367–1374.

de Wijk, R. A., Janssen, A. M., & Prinz, J. F. (2011). Oral movements and the perception of semi-solid foods. *Physiology & Behavior*, *104*(3), 423–428. https://doi.org/10.1016/j.physbeh.2011.04.037

Degrandi-Contraires, É., Beaumont, A., Restagno, F., Weil, R., Poulard, C., & Léger, L. (2013). Cassie-Wenzel–like transition in patterned soft elastomer adhesive contacts. *EPL (Europhysics Letters)*, *101*(1), 14001. https://doi.org/10.1209/0295-5075/101/14001

Foegeding, E. A., Stieger, M., & van de Velde, F. (2017). Moving from molecules, to structure, to texture perception. *Food Hydrocolloids*, *68*, 31–42. https://doi.org/10.1016/j.foodhyd.2016.11.009

Galén, S., & Jost-Brinkmann, P.-G. (2010). B-mode and M-mode Ultrasonography of Tongue Movements during Swallowing. *Journal of Orofacial Orthopedics / Fortschritte Der Kieferorthopädie*, *71*(2), 125–135. https://doi.org/10.1007/s00056-010-9928-8

Hiiemae, K. M. (2004). Mechanisms of food reduction, transport and deglutition: how the texture of food affects feeding behavior. *Journal of Texture Studies*, *35*(2), 171–200.

Hsiao, M.-Y., Chang, Y.-C., Chen, W.-S., Chang, H.-Y., & Wang, T.-G. (2012). Application of ultrasonography in assesing oropharyngeal dysphagia in stroke patients. *Ultrasound in Medicine & Biology*, *38*(9), 1522–1528. https://doi.org/10.1016/j.ultrasmedbio.2012.04.017

Hutchings, J. B., & Lillford, P. J. (1988). The Perception of Food Texture - the Philosophy of the Breakdown Path. *Journal of Texture Studies*, *19*(2), 103–115. https://doi.org/10.1111/j.1745-4603.1988.tb00928.x

Kim, J.-H., & Kim, M.-S. (2012). Lateral pharyngeal wall motion analysis using ultrasonography in stroke patients with dysphagia. *Ultrasound in Medicine & Biology*, *38*(12), 2058–2064. http://dx.doi.org/10.1016/j.ultrasmedbio.2012.07.028

Mantelet, M., Panouille, M., Boue, F., Bosc, V., Restagno, F., Souchon, I., & Mathieu, V. (2019). Impact of sol-gel transition on the ultrasonic properties of complex model foods: Application to agar/gelatin gels and emulsion filled gels. *Food Hydrocolloids*, *87*, 506–518. https://doi.org/10.1016/j.foodhyd.2018.08.021

Mantelet, M., Restagno, F., Souchon, I., & Mathieu, V. (2020). Using ultrasound to characterize the tongue-food interface: An in vitro study examining the impact of surface roughness and lubrication. *Ultrasonics*, *103*, 106095. https://doi.org/10.1016/j.ultras.2020.106095

McEvoy, H., Ross-Murphy, S. B., & Clark, A. H. (1985). Large deformation and ultimate properties of biopolymer gels: 2. Mixed gel systems. *Polymer*, *26*(10), 1493–1500. https://doi.org/10.1016/0032-3861(85)90082-5

Panouillé, M., Saint-Eve, A., & Souchon, I. (2016). Instrumental methods for bolus characterization during oral processing to understand food perceptions. *Current Opinion in Food Science*, *9*, 42–49. https://doi.org/10.1016/j.cofs.2016.05.002

Peng, C.-L., Jost-Brinkmann, P.-G., Miethke, R.-R., & Lin, C.-T. (2000). Ultrasonographic measurement of tongue movement during swallowing. *Journal of Ultrasound in Medicine*, *19*(1), 15–20.

Pramanik, R., Osailan, S. M., Challacombe, S. J., Urquhart, D., & Proctor, G. B. (2010). Protein and mucin retention on oral mucosal surfaces in dry mouth patients. *European Journal of Oral Sciences*, *118*(3), 245–253.

Rommel, N., & Hamdy, S. (2016). Oropharyngeal dysphagia: manifestations and diagnosis. *Nature Reviews Gastroenterology & Hepatology*, *13*(1), 49–59. https://doi.org/10.1038/nrgastro.2015.199

Santagiuliana, M., Piqueras-Fiszman, B., van der Linden, E., Stieger, M., & Scholten, E. (2018). Mechanical properties affect detectability of perceived texture contrast in heterogeneous food gels. *Food Hydrocolloids*, *80*, 254–263. https://doi.org/10.1016/j.foodhyd.2018.02.022

Shull, K. R. (2002). Contact mechanics and the adhesion of soft solids. *Materials Science and Engineering: R: Reports*, *36*(1), 1–45. https://doi.org/10.1016/S0927-796X(01)00039-0

Stokes, J. R., Boehm, M. W., & Baier, S. K. (2013). Oral processing, texture and mouthfeel: From rheology to tribology and beyond. *Current Opinion in Colloid & Interface Science*, *18*(4), 349–359. https://doi.org/10.1016/j.cocis.2013.04.010

Stone, M. (2005). A guide to analysing tongue motion from ultrasound images. *Clinical Linguistics & Phonetics*, *19*(6–7), 455–501. https://doi.org/10.1080/02699200500113558

Szczesniak, A. S. (2002). Texture is a sensory property. *Food Quality and Preference*, *13*(4), 215–225.

Uemori, N., Kakinoki, Y., Karaki, J., & Kakigawa, H. (2012). New method for determining surface roughness of tongue. *Gerodontology*, *29*(2), 90–95. https://doi.org/10.1111/j.1741-2358.2011.00509.x

Weng, C.-K., Chien, J.-W., Lee, P.-Y., & Huang, C.-C. (2017). Implementation of a wearable ultrasound device for the overnight monitoring of tongue base deformation during obstructive sleep apnea events. *Ultrasound in Medicine & Biology*, *43*(8), 1639–1650. http://dx.doi.org/10.1016/j.ultrasmedbio.2017.04.004

Figure captions list

Figure 1: (a) Experimental set-up. (b) Schematic representation of the set-up with a typical US *rf* signal composed of two echoes E_0 and E_1 respectively corresponding to the reflections of the US waves at the interface between the TMS and the food gel, and between the food gel and the artificial palate. (c) M-mode image describing the evolutions of the US response of the system during a compression. The color map corresponds to the amplitude of the *rf* signals (arbitrary units, from blue to yellow).

Figure 2: (a) Means and standard deviations of R^* before the beginning of the compression (ε=0) of three types of gels ((a_1) Ge_7, (a_2) $Ge_{3.5}$ and (a_3) $Ag_{0.3}$) on the different TMSs. (b) Variations of ΔR^* during the compression of three types of gels ((b_1) Ge_7, (b_2) $Ge_{3.5}$ and (b_3) $Ag_{0.3}$) on the different TMSs. The results were obtained under dry lubrication conditions.

Figure 3: For the four gelatin dominant gels ($Ge_{3.5}$, $Ag_{0.3}Ge_{3.5}$, $Ag_{0.7}Ge_{5.85}$ and Ge_7): (a) variations of the force F applied during the compression, (b) variations of ΔR^* during the compression, (c) variations of R^* before the beginning of the compression as a function of the Young's modulus (error bars corresponding to standard deviations and a broken line draws the linear regression for indicative purpose). The results were obtained with $R_1\beta_1$ under dry lubrication conditions.

Figure 4: For the three agar dominant gels ($Ag_{0.3}$, $Ag_1Ge_{0.75}$ and $Ag_{1.8}$): (a) variations of the force F applied during the compression, (b) variations of ΔR^* during the compression, (c) variations of R^* before the beginning of the compression as a function of the Young's modulus (error bars corresponding to standard deviations and a broken line draws the linear regression for indicative purpose). The results were obtained with $R_1\beta_1$ under dry lubrication conditions.

Figure 5: For the four lubrication levels, variations of ΔR^* during the compression of two types of food gels on two types of TMSs: (a_1) Ge_7 and $R_0\beta_0$, (a_2) Ge_7T and $R_0\beta_0$, (b_1) Ge_7 and $R_1\beta_2$ and (b_2) Ge_7T and $R_1\beta_2$.

Tables

Table 1 – Description of the gels in terms of dominant polymer (either agar or gelatin), composition (all of them containing 15 wt% of sucrose), and Young's modulus (average ± standard deviation).

Gel	Dominant Polymer	Composition (wt%)				Young's modulus (kPa)
		Water	Agar	Gelatin	TWEEN 20	
$Ag_{0.3}$	Agar	84.7	0.3	-	-	4.2 ± 3.2
$Ag_1Ge_{0.75}$	Agar	84.25	1	0.75	-	58.4 ± 14.7
$Ag_{1.8}$	Agar	83.3	1.8	-	-	132.0 ± 9.7
$Ge_{3.5}$	Gelatin	81.5	-	3.5	-	2.2 ± 0.4
$Ag_{0,3}Ge_{3,5}$	Gelatin	81.2	0.3	3.5	-	12.7 ± 2.9
$Ag_{0,7}Ge_{5.85}$	Gelatin	78.45	0.7	5.85	-	32.1 ± 7.2
Ge_7	Gelatin	78	-	7	-	24.0 ± 2.2
Ge_7T	Gelatin	77.25	-	7	1.5	17.2 ± 1.8

564

Figure 1

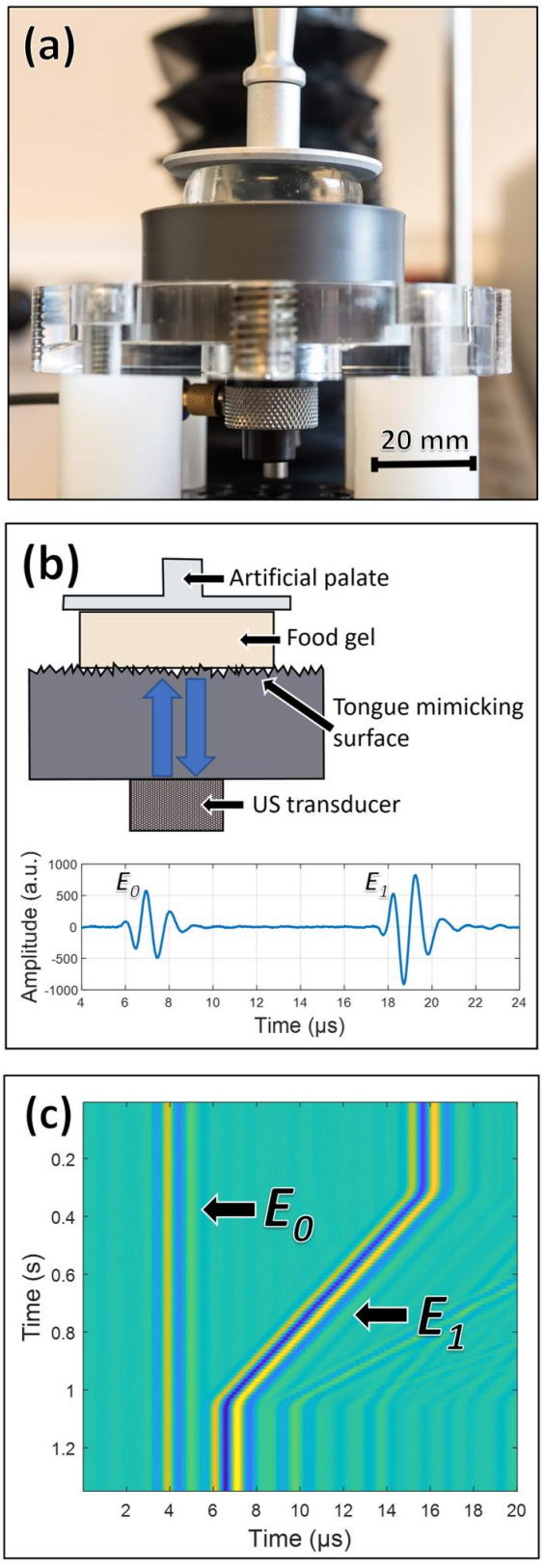

565

566 Figure 2

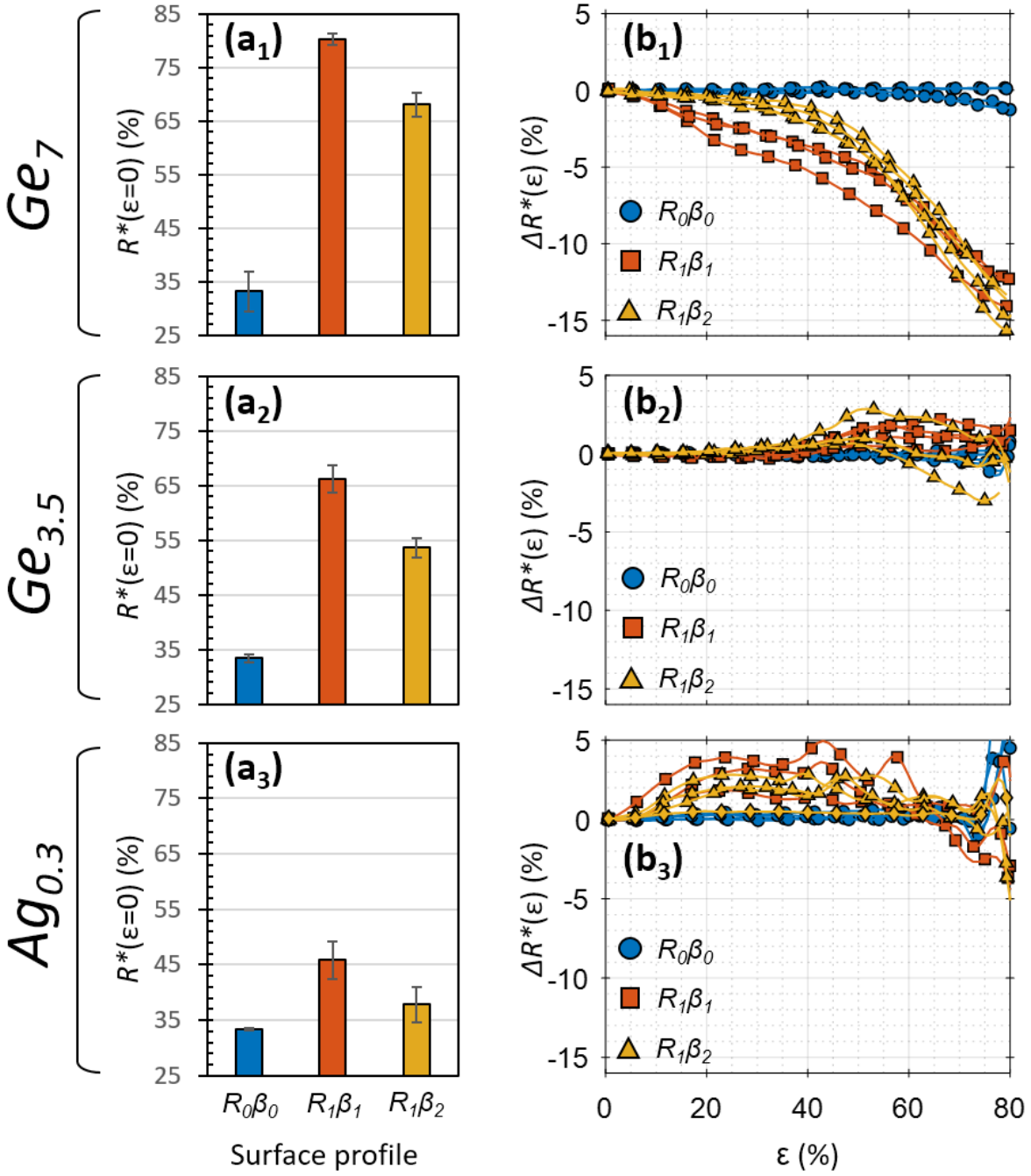

567

568 Figure 3

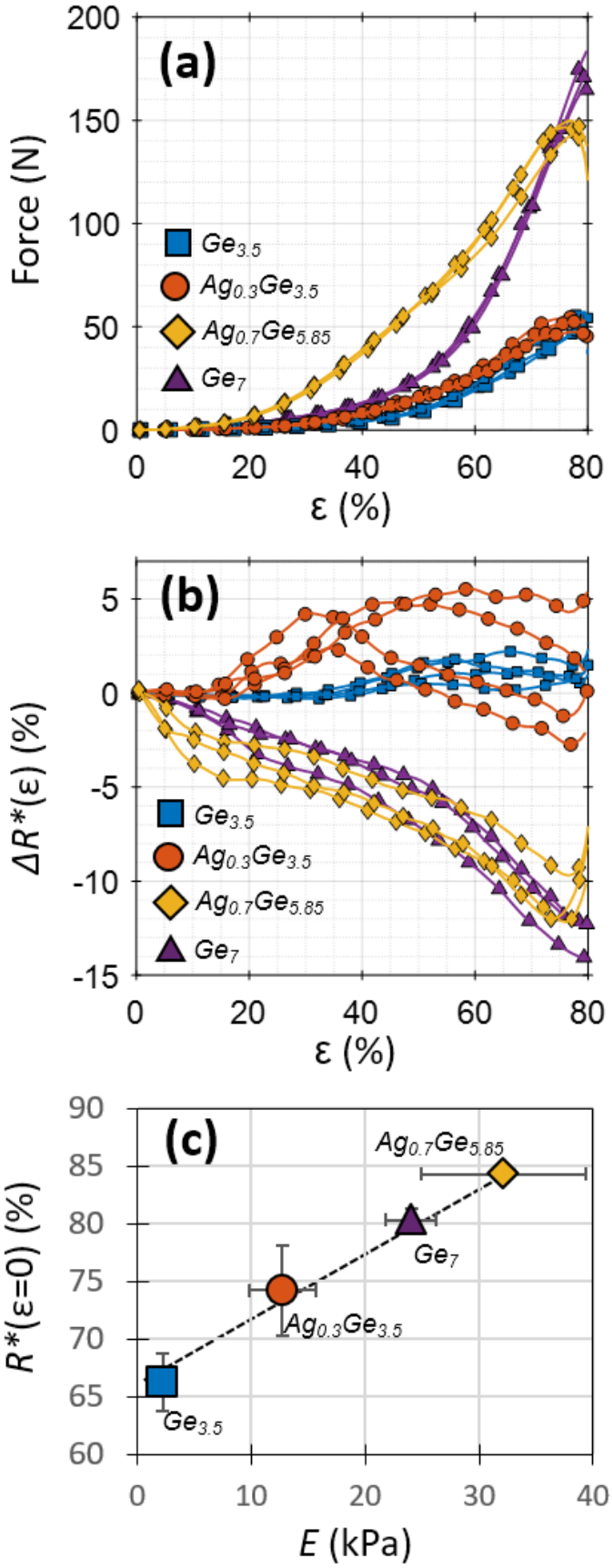

569

Figure 4

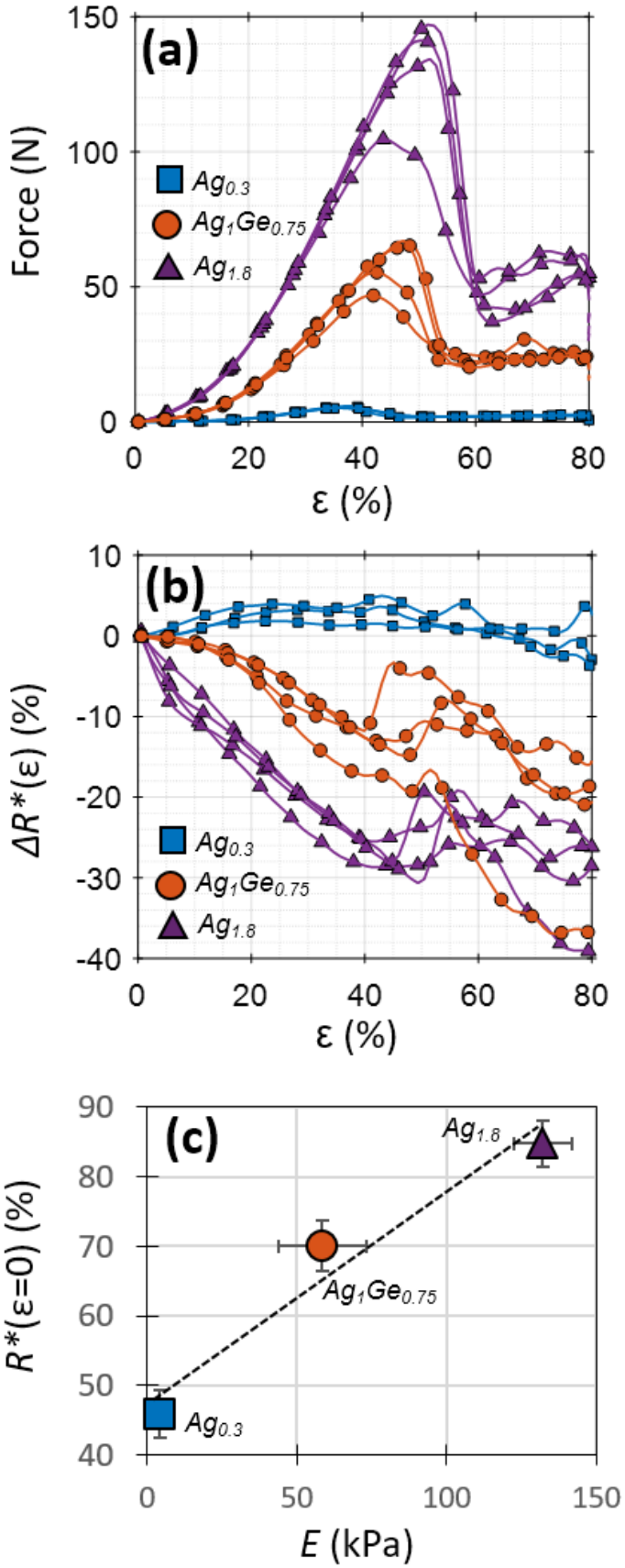
(a)
Force (N)
ε (%)
Ag0.3
Ag1Ge0.75
Ag1.8
(b)
ΔR*(ε) (%)
ε (%)
Ag0.3
Ag1Ge0.75
Ag1.8
(c)
R*(ε=0) (%)
E (kPa)
Ag1.8
Ag1Ge0.75
Ag0.3

572 Figure 5

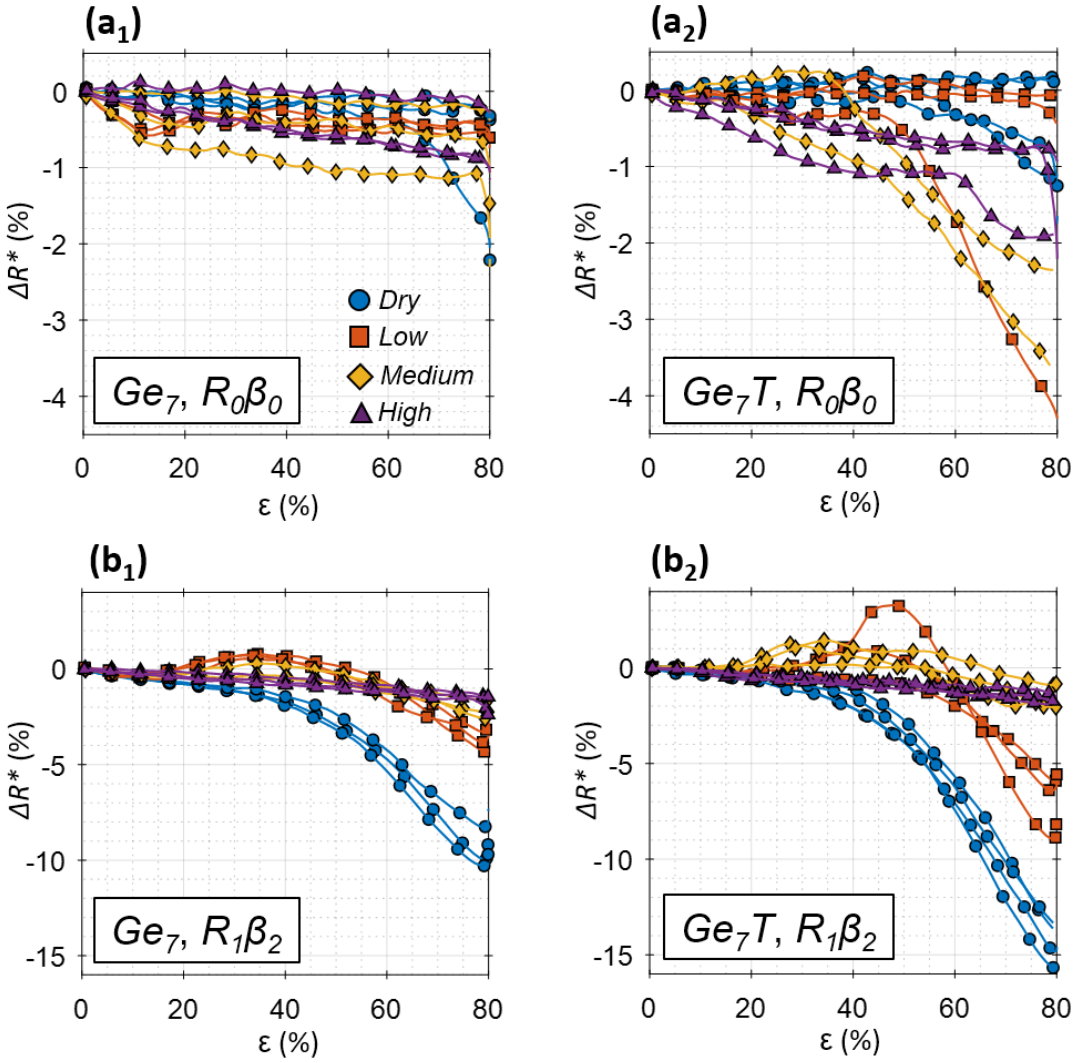

573